TEST VALIDATION OF EXTENSION-TWISTING COUPLED LAMINATES WITH MATCHED ORTHOTROPIC STIFFNESS

C. B. York[1] and K.K. Lee[2]

[1] Singapore Institute of Technology, 10 Dover Drive, Singapore 138683
Christopher.York@singaporetech.edu.sg
www.singaporetech.edu.sg/directory/faculty/christopher-bronn-york

[2] Singapore Polytechnic, 500 Dover Road, Singapore 139651
Lee_kim_kheng@sp.edu.sg
www.sp.edu.sg

Keywords: Extension-Twisting coupling; Hygro-thermally Curvature Stable; Extension-Shearing coupling; Bending-Twisting coupling; Laminate Stacking Sequences.

ABSTRACT

An experimental validation study is presented for three classes of coupled laminate with matching *Extension-Twisting* coupling. The designs also have matching orthotropic stiffness in extension and bending, which have been chosen specifically to investigate the influence of mechanical *Extension-Shearing* and/or *Bending-Twisting* on the performance of *Extension-Twisting* coupled designs under axial tension loads. All designs are hygro-thermally curvature stable (HTCS) or warp-free.

1 INTRODUCTION

This article focuses on the experimental validation of recently identified laminates [1-3] possessing HTCS properties [4-8]. The identification of stacking sequence configurations which satisfy the HTCS condition allows a broad range of exotic mechanical coupling attributes to be exploited without the complicating issue of thermal distortions, which are an inevitable consequence of the high temperature curing process.

Relatively few articles [8] have considered properties beyond isolated *Extension-Twisting* coupling, although it should be noted that *Extension-Twisting* coupled designs also possess an inseparable *Shearing-Bending* coupling counterpart, but this is not active under axial tension loading.

Coupled laminates are described here in terms of their response to various combinations of force and moment resultants, from either mechanical, thermal and/or moisture effects, using a cause and effect relationship. A laminate is therefore described as an *E-S* laminate if extension (*E*) causes a shearing (*S*) effect and is said to possess *Extension-Shearing* coupling. If bending (*B*) causes a twisting (*T*) effect, the laminate is described as a *B-T* laminate and is said to possess *Bending-Twisting* coupling. The four characters *E*, *S*, *B*, and *T* can be used in any combination to describe cause and effect relationship in all coupled laminates [1]; noting that each cause and effect pair is reversible.

Stacking sequence configurations for HTCS laminates have been identified [2] in nine of twenty-four classes of coupled laminate with standard ply angle orientations ±45, 0 and 90°. All arise from the judicious re-alignment of the principal material axis of laminates possessing *Bending-Extension* and *Twisting-Shearing* or *B-E-T-S* coupling, or additionally possessing *Bending-Twisting*, i.e., *B-E-T-S*;*B-T* coupling. The off-axis alignments of these two parent classes then give rise to the other more complex combinations, which include: *Extension-Shearing* or *E-S* coupling; *Bending-Extension* and *Twisting-Shearing* or *B-E-T-S* coupling or; *Extension-Bending*, *Shearing-Bending*, *Extension-Twisting* and *Shearing-Twisting* or *E-B-S-B-E-T-S-T*.

The challenge here is to identify whether any of these complex mechanical coupling properties are of practical significance. In recent years, there has been a significant increase in the use of solid rotor blades, which have so far been associated with unmanned air vehicles, but are now finding application in manned air vehicles, such as the Volocopter; a multicopter, adopting an array of 18 rotor blades.

Extension-Twisting coupled blades can be used to augment lift characteristics through a change in rotor speed, and the resulting extensional (centrifugal) forces.

The design of aero-elastic compliant rotor blades with tailored *Extension-Twisting* coupling, or *E-T* laminate, is an example of one such laminate design that, from a manufacturing perspective, requires either specially curved tooling or hygro-thermally curvature-stable properties in order to remain flat after high temperature curing.

New families of HTCS laminates, with complex mechanical coupling behaviour, are now investigated to assess the performance benefits, such as twist augmentation, from interactions between *Extension*, *Shearing*, *Bending* and *Twisting* on otherwise identical *Extension-Twisting* coupled designs.

The necessary conditions for HTCS laminates are presented, after a summary of the basic relationships between the ABD matrix of stiffness components and lamination parameters, which are adopted to simply the mechanical and thermal characterization. An overview of the database of stacking sequence configurations [2], developed subsequently, is also given.

Stacking sequence configurations within the database are then filtered for matching orthotropic stiffness in extension and bending, as well as coupling behaviour, to reveal designs with additional coupling responses, specifically mechanical *Extension-Shearing* or *E-S* and/or *Bending-Twisting* or *B-T*. The effect of these additional couplings, and how they influence the performance of *Extension-Twisting* or *E-T* coupled designs under axial tension loads is then assessed experimentally for validation of numerical predictions.

The following section provides the basic relationships between the ABD relation and lamination parameters, which help to simply the mechanical and thermal characterization.

2 RELATIONSHIP BETWEEN LAMINATION PARAMETERS AND LAMINATE STIFFNESSES

Lamination parameters provide a convenient way of matching ply angle dependent properties within the database of stacking sequences [2] for a defined number of plies, n, of constant thickness, t, or overall thickness H ($= n \times t$). Elements of the extensional [A], coupling [B] and bending [D] stiffness matrices are related to the lamination parameters and laminate invariants, respectively, by:

$$
\begin{aligned}
A_{11} &= \{U_1 + \xi_1 U_2 + \xi_2 U_3\} \times H \\
A_{12} &= A_{21} = \{-\xi_2 U_3 + U_4\} \times H \\
A_{16} &= A_{61} = \{\xi_3 U_2/2 + \xi_4 U_3\} \times H \\
A_{22} &= \{U_1 - \xi_1 U_2 + \xi_2 U_3\} \times H \\
A_{26} &= A_{62} = \{\xi_3 U_2/2 - \xi_4 U_3\} \times H \\
A_{66} &= \{-\xi_2 U_3 + U_5\} \times H
\end{aligned}
\tag{1}
$$

$$
\begin{aligned}
B_{11} &= \{\xi_5 U_2 + \xi_6 U_3\} \times H^2/4 \\
B_{12} &= B_{21} = \{-\xi_6 U_3\} \times H^2/4 \\
B_{16} &= B_{61} = \{\xi_7 U_2/2 + \xi_8 U_3\} \times H^2/4 \\
B_{22} &= \{-\xi_5 U_2 + \xi_6 U_3\} \times H^2/4 \\
B_{26} &= B_{62} = \{\xi_7 U_2/2 - \xi_8 U_3\} \times H^2/4 \\
B_{66} &= \{-\xi_6 U_3\} \times H^2/4
\end{aligned}
\tag{2}
$$

$$
\begin{aligned}
D_{11} &= \{U_1 + \xi_9 U_2 + \xi_{10} U_3\} \times H^3/12 \\
D_{12} &= D_{21} = \{-\xi_{10} U_3 + U_4\} \times H^3/12 \\
D_{16} &= D_{61} = \{\xi_{11} U_2/2 + \xi_{12} U_3\} \times H^3/12 \\
D_{22} &= \{U_1 - \xi_9 U_2 + \xi_{10} U_3\} \times H^3/12 \\
D_{26} &= D_{62} = \{\xi_{11} U_2/2 - \xi_{12} U_3\} \times H^3/12 \\
D_{66} &= \{-\xi_{10} U_3 + U_5\} \times H^3/12
\end{aligned} \tag{3}
$$

where the laminate invariants are calculated from the reduced stiffness terms, Q_{ij}:

$$
\begin{aligned}
U_1 &= \{3Q_{11} + 3Q_{22} + 2Q_{12} + 4Q_{66}\}/8 \\
U_2 &= \{Q_{11} - Q_{22}\}/2 \\
U_3 &= \{Q_{11} + Q_{22} - 2Q_{12} - 4Q_{66}\}/8 \\
U_4 &= \{Q_{11} + Q_{22} + 6Q_{12} - 4Q_{66}\}/8 \\
U_5 &= \{Q_{11} + Q_{22} - 2Q_{12} + 4Q_{66}\}/8
\end{aligned} \tag{4}
$$

and the reduced stiffness terms are calculated from the material properties:

$$
\begin{aligned}
Q_{11} &= E_1/(1 - \nu_{12}\nu_{21}) \\
Q_{12} &= \nu_{12} E_2/(1 - \nu_{12}\nu_{21}) \\
Q_{22} &= E_2/(1 - \nu_{12}\nu_{21}) \\
Q_{66} &= G_{12}
\end{aligned} \tag{5}
$$

3 HYGRO-THERMALLY CURVATURE-STABLE OR WARP-FREE LAMINATES

The manufacture of any general *Extension-Twisting* coupled laminate presents a particular challenge if such mechanical coupling behaviour is required without the thermal distortions that arise as a consequence of the high temperature curing process. In such cases, the hygro-thermally curvature-stable or thermally warp-free condition offers a manufacturing solution, but with an inevitable restriction in the magnitude of the mechanical coupling.

For extensionally isotropic laminates with standard ply orientations ±45, 0 and 90°, lamination parameters or the equivalent extensional and coupling stiffness elements must satisfy the requirements of Table 1. For orthotropic in-plane properties, the constraints on hygro-thermally curvature-stable laminates may be relaxed in comparison to those stated in Table 1, i.e.: $\xi_1 = \xi_3 = 0$.

Lamination parameters and stiffness relationships with respect to material axis alignment, β.		
$\beta = m\pi/2$ ($m = 0, 1, 2, 3$)	$\beta = \pi/8 + m\pi/2$ ($m = 0, 1, 2, 3$)	$\beta \neq m\pi/2, \pi/8 + m\pi/2$ ($m = 0, 1, 2, 3$)
E-B-S-T	*E-T-S-B*	*E-B-S-B-E-T-S-T*
$\begin{bmatrix} B_{11} & -B_{11} & 0 \\ -B_{11} & B_{11} & 0 \\ 0 & 0 & -B_{11} \end{bmatrix}$	$\begin{bmatrix} 0 & 0 & B_{16} \\ 0 & 0 & -B_{16} \\ B_{16} & -B_{16} & 0 \end{bmatrix}$	$\begin{bmatrix} B_{11} & -B_{11} & B_{16} \\ -B_{11} & B_{11} & -B_{16} \\ B_{16} & -B_{16} & -B_{11} \end{bmatrix}$
$\xi_5 = \xi_7 = \xi_8 = 0$	$\xi_5 = \xi_6 = \xi_7 = 0$	$\xi_5 = \xi_7 = 0$

Table 1 – Conditions for hygro-thermally curvature-stable behaviour in coupled extensionally isotropic laminates with $\xi_1 = \xi_2 = \xi_3 = \xi_4 = 0$.

These conditions correspond to extensional stiffnesses of the following form:

$$\begin{bmatrix} A_{11} & A_{12} & A_{16} \\ A_{12} & A_{11} & -A_{16} \\ A_{16} & -A_{16} & A_{66} \end{bmatrix} \quad (6)$$

which represent the square symmetric form of the extensional stiffness matrix for off-axis material alignment. For coincident material and structural axis alignment, the constraints include $\xi_4 = 0$, which correspond to extensional stiffnesses of the following form:

$$\begin{bmatrix} A_{11} & A_{12} & 0 \\ A_{12} & A_{11} & 0 \\ 0 & 0 & A_{66} \end{bmatrix} \quad (7)$$

Note that the above conditions are independent of the nature of the bending stiffness.

The database of laminate designs [2] contains definitive listings of all forms of coupled HTCS laminate. These are presented in symbolic form, together with non-dimensional parameters; making each configuration independent of both material properties and fibre orientations. Fibre directions are required to have a specific angle separation to achieve HTCS properties and whilst commonly adopted angles are used here, i.e., 0, ±45 and 90°, other angle separations have been shown to be possible.

The choice of 16 ply laminates for the experimental test allows a rich design space for stiffness matching.

The design space representing *E-B*-*S-T*;*B-T* coupled extensionally isotropic laminates contains 6, 280, 23,652 and 2,379,722 sequences with 8, 12, 16 and 20 plies, respectively. Whilst extensional isotropy is retained, *Bending-Twisting* coupling is present for all off-axis alignments. However, there are a number of exceptions: 3, 10 and 126 cases arise for 8-, 12- and 16-ply laminates for which off-axis alignment $\beta = \pi/8 + m\pi/2$ (m = 0, 1, 2, 3), renders the laminate uncoupled in bending, i.e. $D_{16} = D_{26} = 0$. The gives rise to the *E-T*-*S-B* coupling properties of interest.

It was from this relatively small group of designs that laminate 1 of Table 2 was chosen.

Ref.	Stacking Sequence, $\beta = 0°$	Coupling, $\beta = 0°$ ($\pi/2$)	Coupling, $\beta = \pi/8$ ($+ \pi/2$)
1	$[-45_2/45_2/0/45/-45/90/45/0/90/-45/90_2/0_2]_T$	*E-B*-*S-T*;*B-T*	*E-T*-*S-B*
2	$[-45/0/45_3/-45_3/90/45/90_2/0/90/0_2]_T$	*E-B*-*S-T*	*E-T*-*S-B*;*B-T*
3	$[-45/45_2/-45/0_3/90_6/0_3]_T$	*E-B*-*S-T*	*E-S*;*E-T*-*S-B*;*B-T*

Table 2 – Laminate designs and mechanical properties, as manufactured, $\beta = 0°$, and as tested, $\beta = \pi/8$.

The choice of the comparator designs was then sought with matching orthotropic as well as coupling stiffness properties.

The design space representing *E-B*-*S-T* coupled laminates with extensional isotropy, contains 8, 264 and 17,118 sequences with 12, 16 and 20 plies, respectively. Within this design space exist 8 designs, containing 16 plies, that can be described as quasi-homogeneous, i.e., $D_{ij} = A_{ij}H^2/12$. All designs retain isotropic extensional properties, but with the exception of the 8 quasi-homogeneous solutions, develop *Bending-Twisting* coupling for any off-axis material alignment. The gives rise to the *E-T*-*S-B*;*B-T* coupling properties of interest, representing Laminate 2 of Table 2

The design space representing *E-B*-*S-T* coupled laminates with extensional orthotropy contains 6, 524, and 35,610 with 12, 16 and 20 plies, respectively. Properties for off-axis alignment $\beta = \pi/8 + m\pi/2$, (m = 0, 1, 2, 3) therefore give rise to *Extension-Shearing* and Bending-Twisting coupling for any off-axis material alignment. This gives rise to the *E-S*;*E-T*-*S-B*;*B-T* laminate characteristics of interest, representing Laminate 3 of Table 2.

4 NUMERICAL SIMULATION

4.1 FINITE ELEMENT MODELLING

A non-linear Finite Element (Riks) analysis is used [9] to predict the *Extension-Twisting* coupling response for comparison with the experimental tests that follow. The FE model is created to match the laminate with dimensions 240 x 24 x 2.43 mm, using 4-noded shell elements (S4R). A converged solution was obtained with 1mm square elements. One end of the model is constrained to simulate the fully-clamped condition, whilst at the other, extension is permitted in only the loading axis direction together rotational freedom around the same axis. The gauge length was adjusted to 189 mm to match the physical distance between grips, measured after testing from indentations on the specimens by the bevelled edge grips, see Fig. A1.

The Carbon fibre/Epoxy materials (T700HS/SE 84LV) properties match those of the specimens tested, i.e., E_1 = 131 GPa, E_2 = 8.2 GPa, G_{12} = 4.3 GPa and ν_{12} = 0.38. Cured ply thickness varied, ranging between t = 0.158mm – 0.166mm, and giving an overall thickness H = 2.53 – 2.66mm for the laminate designs of Table 2. Abaqus input files are provided in the electronic annex using averaged thicknesses for each of the specimens, gathered from the data presented in Table A1.

Note that *E-S*;*E-T*-*S-B*;*B-T* required addition constraints to enforce *Extension-Twisting* without *Extension-Bending* coupling due to interaction between *E-T* and *B-T* coupling characteristics. This could not be captured experimentally, see Fig. 3, but raises an important questions about the aerodynamic effects, i.e., lift augmentation in a rotating blade, as a result of such a response.

4.1 CONSTITUTIVE RELATIONS

The lamina thickness assumed here was 0.163mm, giving a total laminate thickness of 2.608mm, from which the following ABD matrix for Laminate 1 produced a twist curvature, κ_{xy}, of -0.00188/mm using a load N_x = 208.3 N/mm, equivalent to the 5 kN test load.

$$\begin{bmatrix} 145,037 & 46,339 & 0 & 0 & 0 & 18,648 \\ & 145,037 & 0 & 0 & 0 & -18,648 \\ & & 49,350 & 18,648 & -18,648 & 0 \\ & & & 103,458 & 26,264 & 0 \\ & & & & 60,957 & 0 \\ \textit{Symm} & & & & & 27,297 \end{bmatrix}$$

Laminate 2 produced an augmentation in the twist curvature, κ_{xy}, of 14% above Laminate 1 due to the additional coupling terms D_{16} and D_{26}:

$$\begin{bmatrix} 145,037 & 46,339 & 0 & 0 & 0 & 18,648 \\ & 145,037 & 0 & 0 & 0 & -18,648 \\ & & 49,350 & 18,648 & -18,648 & 0 \\ & & & 103,458 & 26,264 & 15,692 \\ & & & & 60,957 & 5,559 \\ \textit{Symm} & & & & & 27,297 \end{bmatrix}$$

Laminate 3 produced an augmentation in the twist curvature, κ_{xy}, of 57% above Laminate 1 due to the additional coupling terms A_{16} and A_{26} and D_{16} and D_{26}:

$$\begin{bmatrix} 145,037 & 46,339 & 19,068 & 0 & 0 & 18,648 \\ & 145,037 & -19,068 & 0 & 0 & -18,648 \\ & & 49,350 & 18,648 & -18,648 & 0 \\ & & & 103,458 & 26,264 & 12,568 \\ & & & & 60,957 & 7,165 \\ \textit{Symm} & & & & & 27,297 \end{bmatrix}$$

The through thickness stress distributions, representing an unconstrained laminate under axial tension are given Fig. A1. However, it is difficult to predict that one laminate has the a different twist response to the other just by simple inspection.

5 EXPERIMENTAL VALIDATION

Experimental results are presented for a very specific range of thermo-mechanical coupling responses, which focus firstly on thermally stable curvature predictions, which are readily validated experimentally by virtue of the fact the plate specimens remain perfectly flat following the high temperature curing process.

Mechanical test validation was then performed to assess the isolated effects of combined mechanical coupling behaviour for orthotropic stiffness matched laminate configurations, as highlighted in Table 2. Here, each class of coupled laminate is manufactured with standard fibre alignments (0, ±45, 90°) using constant thickness carbon-fibre/epoxy using a standard autoclave curing process. Specimens were then prepared at an off-axis orientation ($\beta = \pi/8$) to the manufacturing axis to induce the desired *Extension-Twisting* coupling behaviour.

Experimental validation of *Extension-Twisting* behaviour was performed using an MTS BIONIX 25 kN axial-torsional machine, see Fig. 1. A 0.5 mm/min extension rate was used to introduce quasi-static loading. The hydraulic grips were set to 6.2 MPa (900 psi) to prevent slippage of the specimen.

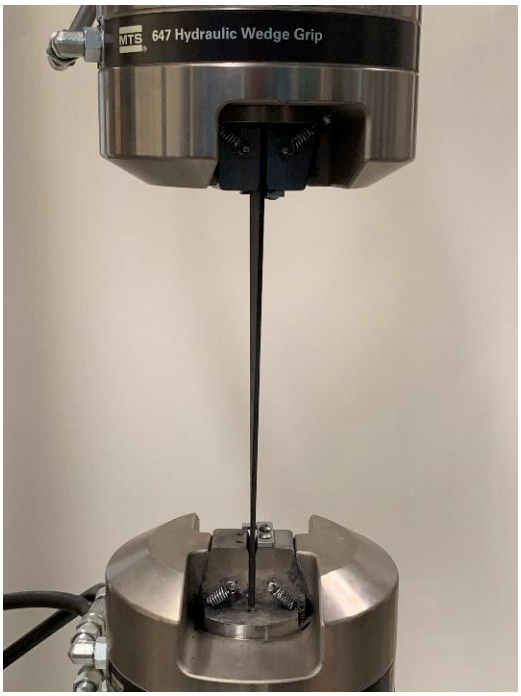

Fig. 1. MTS BIONIX 25kN axial-torsional machine, illustrating Laminate 1 under test (4.9kN tension load), resulting in a twist angle of 8.46°.

6 RESULTS AND DISCUSSION

Extension-Twisting coupling behaviour exists together with *Shearing-Bending* coupling at the laminate level characteristic. However, *Shearing-Bending* coupling is not active under tension loading. However, for the more complex coupling behaviour that we see in the other laminates (2 and 3) of Table 2, there is clear evidence that coupling interactions exist, which serves to augment the twisting response. *Bending-Twisting* coupling in laminate 2 results in an interaction with *Shearing-Bending* and addition of *Extension-Shearing* coupling in laminate 3 results in further interaction with *Shearing-Bending*. These responses are constrained in the experimental test and therefore lead to an increase in the twisting response of the specimen. At a applied load of 4.9kN, average twist angles for Laminates 1, 2 and 3 were, respectively, 8.5, 9.5 and 12.6°.

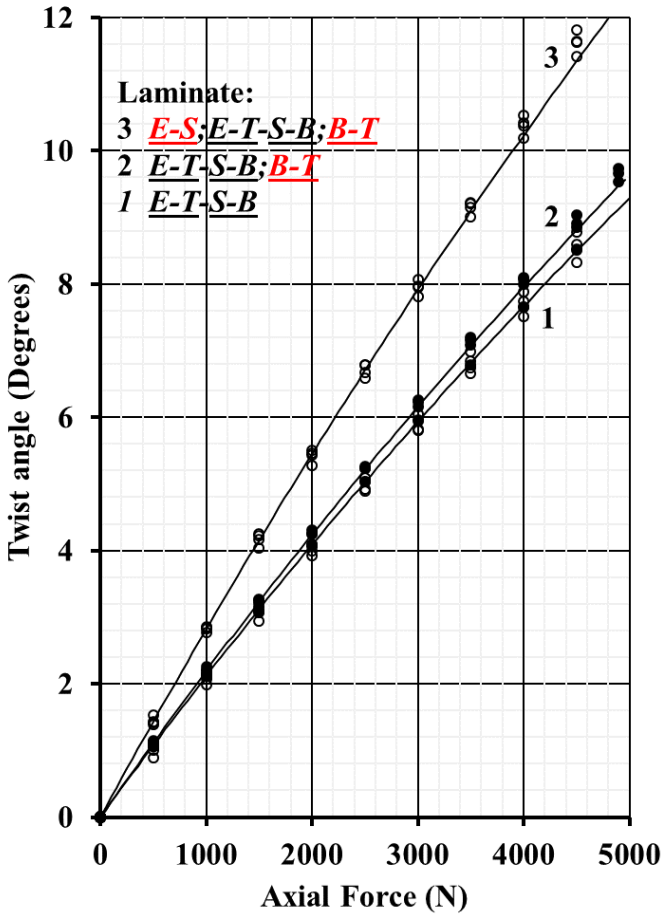

Fig. 2. Twist response of Laminates 1 – 3 of Table 2 under axial tension for laminate stacking sequences of Table 1 with $\beta = \pi/8$.

Based on test results (open circles) for Laminate 1, illustrate in Fig. 2, the measured angles correspond to a twist augmentation, above the *Extension-Twisting* coupled baseline design, of 13% and 47%, for Laminate 2 (filled circles) and Laminate 3, respectively. These results can be seen to agree closely with the non-linear Finite element simulations. However, twist response proved to be highly sensitive to laminate thicknesses, and required careful matching due to the significant thickness variation between test specimens, see Table A1. Width variations were also accounted for due to inaccuracies in the water jet cutting. Some overlap in the test results is evident. The twist augmentations can also be seen to agree well with predictions from the constitutive equations, which suggests that the specimen was of sufficient length that the grips had a rather limited far field effect.

Relaxing the effect of the grips can be captured only through numerical modelling and indeed revealed that Laminate 3 does exhibit some secondary *Bending* and *Shearing* in addition to the *Extension-Twisting* behaviour as indicated by the movement of the reference node, denoted by a cross

in perspective views of the specimen deformation simulation in Fig. 3. The reference node, through which load was applied and displacement/rotation measured, was attached through rigid elements to the top edge of the plate to simulate the hydraulic grips of the MTS BIONIX, see Fig. 1.

(a) (b)

Fig. 3. Twist response for laminate 3: (a) with and; (b) without deflection constraints applied to the loaded end to simulate the hydraulic grip movement of the experiment.

9 CONCLUSIONS

This study has presented experimentally validated numerical predictions of Hygro-Thermally Curvature Stable designs with *Extension-Twisting* coupled laminates to which combined mechanical couple behaviour has been assessed.

The addition of secondary mechanical coupling has been found augment substantially the *Extension-Twisting* coupling response under uniaxial axial tension. Indeed the experimental results have demonstrated twist augmentation above the *Extension-Twisting* coupled baseline design of approximately 13% when combined with *Bending-Twisting* coupling and approximately 47% when combined with both *Bending-Twisting* and *Extension-Shearing*.

Numerical simulations, beyond the scope of the experimentally validated results, suggest that rotating blades may develop tip bending and shearing deformation, which may possibly lead to interesting effects in the aerodynamics.

ACKNOWLEDGEMENTS

The authors gratefully acknowledge the support of the following people in connection with composite manufacture, specimen preparation and test: Tommy Kim Wee Goh, Run An Ong, Loogeswaran Enrique Arumugam, Angela Shi Ying Tham and Linyun Zhang.

REFERENCES

[1] C. B. York, A unified approach to the characterization of coupled composite laminates: Benchmark configurations and special Cases, *J. Aero. Eng., ASCE*, **23**, 2010, pp. 219-242.

[2] C. B. York, Unified approach to the characterization of coupled composite laminates: Hygro-thermally curvature-stable configurations, *International Journal of Structural Integrity*, **2**, 2011, pp. 406-436.

[3] C. B. York, Coupled Quasi-Homogeneous Orthotropic Laminates, *Mechanics of Composite Materials*, **47**, 2011, pp. 405-426.

[4] H. P Chen, Study of hygrothermal isotropic layup and hygrothermal curvature-stable coupling composite laminates, *Proceedings of the 44th AIAA/ASME/ASCE/AHS/ASC Structures, Structural Dynamics, and Materials Conf*erence, Paper No. AIAA-2003-1506, 2003.

[5] P. M. Weaver, Anisotropic Laminates that Resist Warping during Manufacture, *Proceedings of the 15th International Conference on Composite Materials*, Durban, S. Africa, 2005.

[6] R. J. Cross, R. A. Haynes and E. A. Armanios. "Families of hygrothermally stable asymmetric laminated composites." Journal of Composite Materials, **42**, 2008, pp. 697-716.

[7] G. Verchery, Search for Thermally Stable Laminates, *Proceedings of the 15th Composites Durability Workshop*, Kanazawa, Japan, 2010.

[8] R. A. Haynes and E. A. Armanios, Hygrothermaly stable extension-twist coupled laminates with bending-twist coupling, *Proceedings of the ASME 2010 International Mechanical Engineering Congress & Exposition IMECE2010*, Vancouver, British Columbia, Canada, 2010.

[9] ABAQUS/Standard, Version 6.14. Dassault Systèmes Simulia Corp. 2018.

APPENDIX

		Specimen thickness				Specimen width			
Position:	Top	2.43	2.62	2.59	2.58	24.05	24.09	24.08	24.05
	Middle	2.56	2.62	2.63	2.63	24.07	24.06	24.15	24.16
	Bottom	2.60	2.66	2.70	2.64	24.02	24.09	24.12	24.10
Laminate:	Average *H*	2.53	2.63	2.64	2.62	24.05	24.08	24.11667	24.10
Ply:	Average *t*	0.158	0.165	0.165	0.164				

(a) – Laminate 1

		Specimen thickness				Specimen thickness			
Position:	Top	2.53	2.57	2.62	2.66	24.05	24.09	24.08	24.05
	Middle	2.61	2.65	2.69	2.66	24.07	24.06	24.15	24.16
	Bottom	2.61	2.67	2.70	2.70	24.02	24.09	24.12	24.10
Laminate:	Average *H*	2.58	2.63	2.67	2.67	24.05	24.08	24.12	24.10
Ply:	Average *t*	0.161	0.164	0.167	0.167				

(b) – Laminate 2

		Specimen thickness				Specimen thickness			
Position:	Top	2.61	2.69	2.64	2.7	23.64	23.8	23.86	23.57
	Middle	2.64	2.66	2.63	2.67	23.57	23.83	23.59	23.49
	Bottom	2.66	2.66	2.62	2.68	23.67	23.82	23.74	23.64
Laminate:	Average *H*	2.64	2.67	2.63	2.68	23.63	23.82	23.73	23.57
Ply:	Average *t*	0.165	0.167	0.164	0.168				

(c) – Laminate 3

Table A1: Geometry for each of the four samples for each of the three laminate designs of Table 2.

Figure A1 – Gauge length measurement confirmed from indentations on test specimens from bevel edged serrated grips.

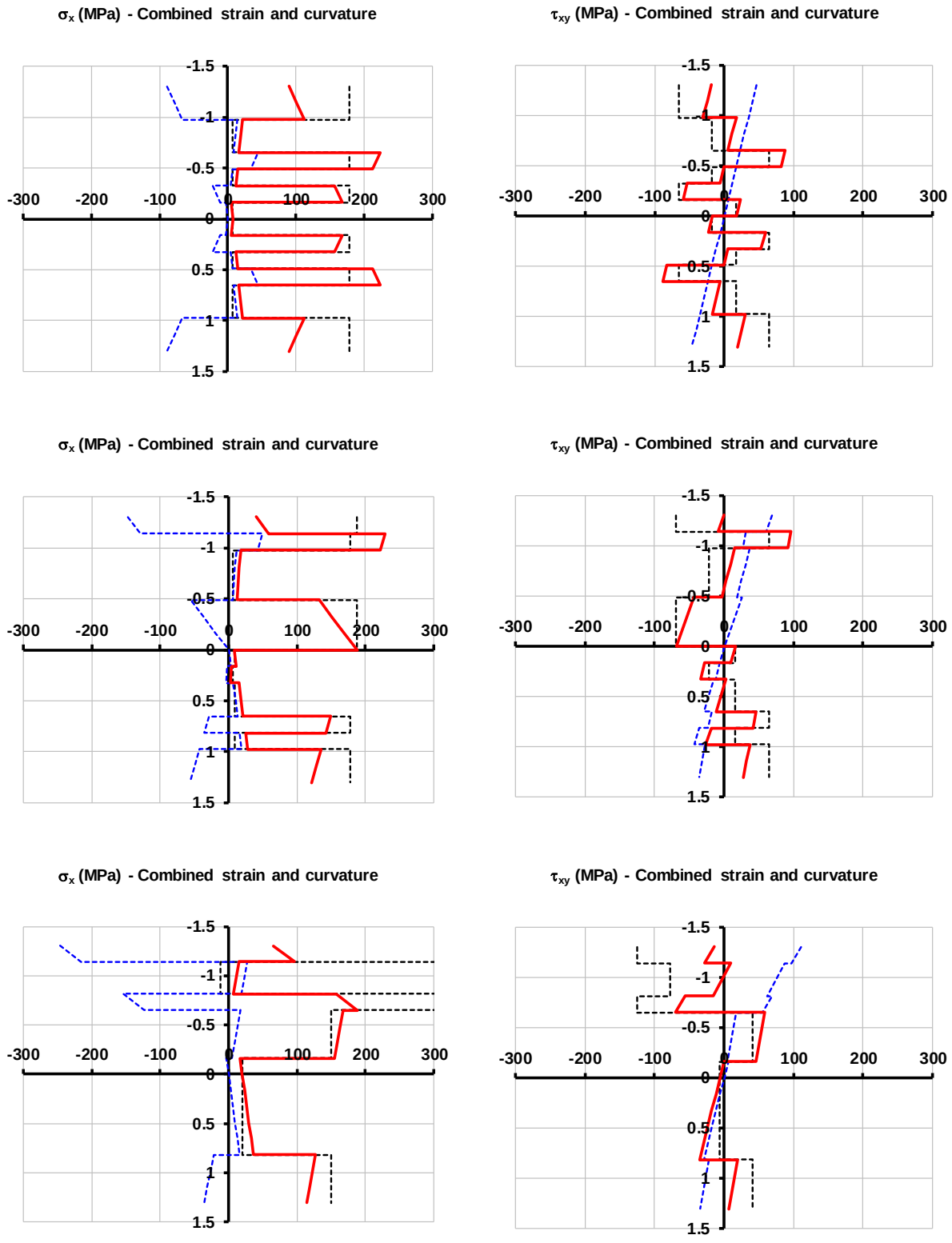

Fig. A2 – Through thickness stress distributions, arising from unconstrained axial tension N_x = 208.3 N/mm, corresponding to axial (σ_x) and shear (τ_{xy}) stress for laminates 1, 2 and 3 in Table 1, (top to bottom) respectively. Axial and bending stresses (broken lines), are shown together with the final stress distribution (solid line).